CHEMISTRY
A European Journal

Accepted Article

Title: High-Throughput Assay for Enantiomeric Excess Determination in 1,2- and 1,3-Diols and Direct Asymmetric Reaction Screening

Authors: Elena G. Shcherbakova, Valentina Brega, Vincent M. Lynch, Tony D. James, and Pavel Anzenbacher

FULL PAPER

High-Throughput Assay for Enantiomeric Excess Determination in 1,2- and 1,3-Diols and Direct Asymmetric Reaction Screening

Elena G. Shcherbakova[a], Valentina Brega[a], Vincent M. Lynch[b], Tony D. James[c], and Pavel Anzenbacher, Jr. *[a]

Abstract: A simple and efficient method for determination of the yield, enantiomeric/diasteriomeric excess (*ee/de*), and absolute configuration of crude chiral diols without the need of work-up and product isolation in a high throughput setting is described. This approach utilizes a self-assembled iminoboronate ester formed as a product by dynamic covalent self-assembly of a chiral diol with an enantiopure fluorescent amine such as tryptophan methyl ester or tryptophanol and 2-formylphenylboronic acid. The resulting diastereomeric boronates display different photophysical properties and allow for fluorescence-based *ee* determination of molecules containing a 1,2- or 1,3-diol moiety. This method has been utilized for the screening of *ee* in a number of chiral diols including atorvastatin, a statin used for the treatment of hypercholesterolemia. Noyori asymmetric hydrogenation of benzil was performed in a highly parallel fashion with errors <1% *ee* confirming the feasibility of the systematic examination of crude products from the parallel asymmetric synthesis in real time and in a high-throughput screening (HTS) fashion.

Introduction

Chiral diols represent essential structural motifs found in pharmaceuticals,[1] biologically active natural products,[2] synthetic precursors and intermediates,[3] or chiral catalysts/auxiliaries used in a number of asymmetric transformations.[4],[5],[6] Asymmetric dihydroxylation of alkenes,[7],[8] asymmetric hydrogenation of ketones,[9],[10] and dicarbonyl reduction by single enzyme[11] are among the most advantageous synthetic procedures for the preparation of chiral diols. Recent advances in the development of methods for the preparation of 1,2- and 1,3-diols necessitate the development of high-throughput screening techniques for the fast determination of enantiomeric excess (*ee*), which is essential for the optimization of chiral catalysts and libraries of auxiliaries for asymmetric transformations where the ability to analyse a large number of samples in parallel fashion is highly desirable.[12]
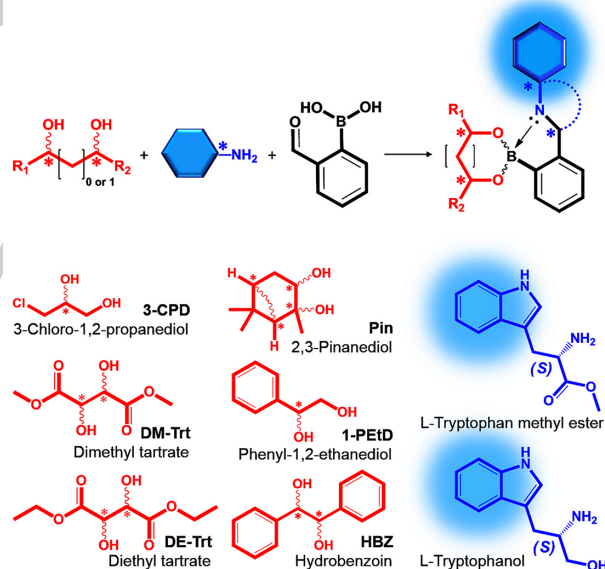
Currently, the most common methods used for the determination of enantiomeric purity involve ^{1}H- and ^{19}F-NMR spectroscopy,[13],[14],[15],[16] circular dichroism (CD),[17],[18],[19],[20] chiral-phase high performance liquid chromatography (HPLC), HPLC coupled with circular dichroism (HPLC-CD), or chiral gas chromatography (GC).[21] Such techniques are, however, better suited for serial analyses while the need for the simple parallel platforms remains largely unmet. For this reason, the HTS methods allowing for the use of simple commercial instrument platforms in conjunction with multi-well formats are sought.[18]

We have recently reported the first fluorescence-based assay for the rapid parallel determination of the *ee* value of amines and amine derivatives utilizing the dynamic covalent self-assembly approach.[22],[23] Our new approach for the determination of the *ee* of chiral diols (Figure 1 bottom) is based on the dynamic covalent self-assembly[24],[25],[26],[27] of an enantiomerically pure fluorescent amine reporter with 2-formylphenylboronic acid (FPBA) and a molecule containing a 1,2- or 1,3-diol moiety (Figure 1 top).

[a] E. G. Shcherbakova, Dr. V. Brega, Prof., Dr. P. Anzenbacher, Jr
Department of Chemistry
Bowling Green State University
Bowling Green, OH, USA 43403
E-mail: pavel@bgsu.edu
[b] Dr. V. M. Lynch
Department of Chemistry
University of Texas at Austin
Austin, TX 78712, USA
[c] Prof., Dr. T. D. James
Department of Chemistry, University of Bath
Claverton Down, Bath BA2 7AY, UK

Supporting information for this article is given via a link at the end of the document.

Figure 1. Concept of dynamic covalent self-assembly for enantiomeric excess determination in chiral diols and asymmetric reaction characterization. **Top**: 1,2- or 1,3-Diols self-assemble with an enantiomerically pure fluorescent amine reporter and 2-formylphenylboronic acid. **Bottom**: The diol analytes/substrates and fluorescent amines used in this study.

FULL PAPER

Results and Discussion

The successful formation of the iminoboronate ester/oxazolidine complexes was confirmed by matrix-assisted laser desorption/ionization (MALDI) mass spectrometry (see the Supplemental Information), single-crystal X-ray diffraction analysis, and fluorescence spectroscopy. As expected, the reaction between L-tryptophanol (1,2-amino alcohol), FPBA, and a diol yields an oxazolidine boronate ester.[26] Figure 2 shows the X-ray crystal structures of the two diastereomeric oxazolidine
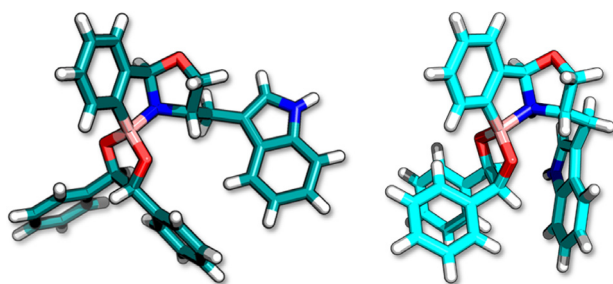
boronate esters self-assembled from L-tryptophanol, FPBA and (R,R)- or meso-hydrobenzoin in a 1:1:1 stoichiometry.

Figure 2. Crystal structures of oxazolidine boronate esters self-assembled from FPBA, L-tryptophanol, and (R,R)-HBZ (left), and meso-HBZ (right).

The choice of tryptophan derivatives was motivated by the potential for bright fluorescence. The variation of the spectroscopic properties originate from different geometrical arrangement around the boron center to induce an intramolecular collisional quenching. Due to a strong enantiomer-induced fluorescence signal (amplification or quenching), fluorometric titrations enable a quantitative estimation of chiral enrichment in a diverse set of diols (Figure 1 bottom). As chiral fluorescent reporter moieties, we selected enantiomerically pure L-tryptophan methyl ester and L-tryptophanol (Table 1).

Table 1. Affinity constants K_a ($\times 10^6$ M^{-1}) a corresponding to L-tryptophan methyl ester (L-TrpOMe) and L-tryptophanol (L-TrpOH) based complexes with selected chiral diols[a].

	K_a ($\times 10^6$ M^{-1})	
	L-TrpOMe	L-TrpOH
(S)-α-Glycerol chlorohydrin	1.65	0.64
(R)-α-Glycerol chlorohydrin	0.47	4.33
(S)-(+)-Phenylethylene glycol	0.47	4.72
(R)-(−)-Phenylethylene glycol	1.39	3.15
(+)-Dimethyl L-tartrate	1.04	4.07
(−)-Dimethyl D-tartrate	0.96	4.50
(+)-Diethyl L-tartrate	1.10	7.71
(−)-Diethyl D-tartrate	0.36	5.15
(1S,2S,3R,5S)-(+)-Pinanediol	0.20	2.31
(1R,2R,3S,5R)-(−)-Pinanediol	0.32	11.0
(S,S)-(−)-Hydrobenzoin	1.83	8.40
meso-Hydrobenzoin	0.45	3.37
(R,R)-(+)-Hydrobenzoin	0.49	0.40
(3S,5S)-Atorvastatin	0.38	2.60
(3R,5R)-Atorvastatin	2.34	3.34

[a] All titrations were performed in acetonitrile/water (5% v/v). The K_as were calculated based on the change in fluorescence intensity upon the addition of each chiral diol. The K_as were calculated using non-linear least-square fitting, errors of the fitting were < 20%.

Figure 3 shows the fluorometric titration profiles of the enantiomeric pair of diethyl tartrate upon the formation of the oxazolidine boronate ester with L-tryptophanol. The formation of diasteriomeric complexes exhibit high association constants with both enantiomers of diethyl tartrate (Figure 3, and Table 1), but (+)-diethyl-L-tartrate displays ca. 20-fold stronger fluorescence amplification. The graph insets show the nonlinear least-square fit of the data using a 1:1 binding model. The respective association constants were (K_a, M^{-1}) $K_{a(L)} = 7.7 \times 10^6$ M^{-1} and $K_{a(D)} = 5.2 \times 10^6$ M^{-1} for (+)-diethyl-L-tartrate and (-)-diethyl-D-tartrate, respectively.
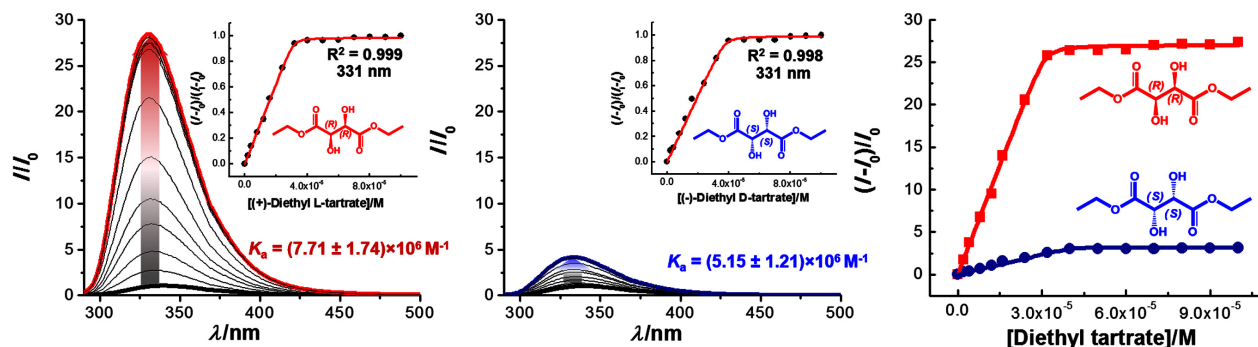

Figure 3. Fluorescence titrations of L-tryptophanol - FPBA (1:1, 40 μM) with diethyl-tartrate enantiomers (0-100 μM) in MeCN. λ_{ex} = 280 nm. Left: (+)-diethyl-L-tartrate; Center: (−)-diethyl-D-tartrate; Right: Isotherms show the difference in signal amplification for the two diethyl tartrate esters (λ_{em} = 330 nm)

FULL PAPER

As another example of the utility of the present method we show the *ee* analysis of the statin-type blockbuster drug atorvastatin used for the treatment of hypercholesterolemia[28],[29] and the prevention of cardiovascular diseases.[30],[31]

Atorvastatin exists in four stereoisomers, but commercialized is only the enantiopure (3*R*,5*R*)-7-[2-(4-fluorophenyl)-3-phenyl-4-(phenylcarbamoyl)-5-propan-2-ylpyrrol-1-yl]-3,5-dihydroxyheptanoic acid form.[11],[32] Figure 4 bottom shows that addition of (3*S*,5*S*)-atorvastatin, the inactive enantiomer,[33],[34] to the FPBA/L-tryptophanol mixture induces an intensity enhancement of L-tryptophanol florescence. Conversely, the fluorescence of the L-tryptophanol is quenched upon the addition of the biologically active (3*R*,5*R*)-atorvastatin (Figure 4 top).
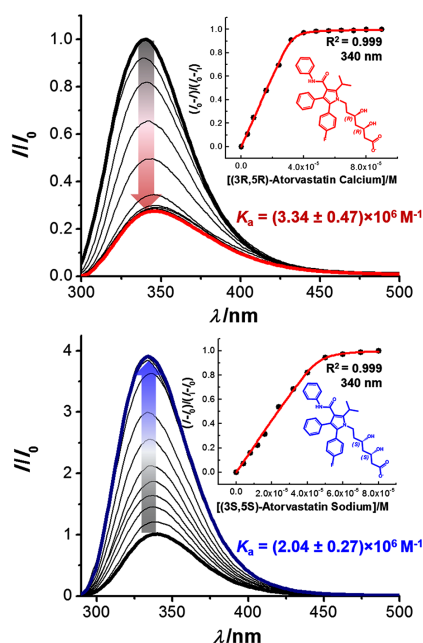

Figure 4. Fluorescence titrations of L-tryptophanol - FPBA (1:1, 40 μM) with atorvastatin enantiomers. Top: stepwise addition of (3*R*,5*R*)-atorvastatin (0-100 μM) in MeCN. λ_{ex} = 280 nm. Bottom: addition of (3*S*,5*S*)-atorvastatin (0-80 μM) in MeCN. λ_{ex} = 280 nm.

Further tests with various enantiomeric diols show that different diols also either quench or amplify the fluorescence albeit to different degrees. The complementarity in association affinities of the complexes, together with the analyte-specific signal amplification/quenching output, indicates that the combination of enantiopure tryptophan methyl ester/tryptophanol based complexes will be suited for recognition and identification using fluorescence-based HTS methods.

First, a qualitative analysis was performed to confirm the ability of the assemblies to differentiate between structurally similar enantiomeric pairs of chiral diols. The fluorescence intensities were recorded using a conventional microplate reader in 384-well plate (16 data clusters/20 repetitions). The response patterns associated with the assemblies were obtained in the form of multivariate data sets. Hence, pattern recognition techniques

such as supervised method linear discriminant analysis (LDA) were used.[35],[36],[37] LDA reduces the dimensionality of the data used to identify the samples and separate the data set into groups of clusters based on similarities in the response data, and to help identify possible patterns and functional relationship between the clusters. The leave-one-out cross-validation protocol confirmed the ability of the tryptophan methyl ester/tryptophanol based fluorescent complexes to differentiate between 7 enantiomeric pairs of chiral diols with 100% correct classification for 320 data points (16 by 20 repetitions).

Figure 5 illustrates the graphical output of LDA where we see a tight grouping of the data points within the individual clusters and a clear segregation of the clusters, which corresponds to large differences in the fluorescence of the various diols and their enantiomers within the large response space defined by the first three canonical factors (F1-F3) of LDA.

The qualitative analysis above confirms that the covalent self-assemblies can be used to recognize a variety of enantiomeric diols using their fluorescence and should allow for the quantitative determination of their *ee*.

An important feature observed in the qualitative analysis (Figure 5 left) of the chiral diols is the distance between the enantiomers that reflects the difference in the fluorescence behavior of the diastereomeric assemblies of the diols. In fact, the larger the distance, the lager the difference between the behavior of the enantiomers. Particularly interesting is the example of hydrobenzoin, for which we tested the *S,S*-, *R,R* and *meso*-form. The clusters corresponding to the three forms are well separated suggesting that a quantitative analysis will be possible.

Next, the loading test of the sensing system was performed using five different diols at various levels of *ee* (0-100%) (Figure 5 right). In the simultaneous high-throughput experiment the 47 data-points with 24 repetitions in each cluster (1128 individual measurements) were dispensed and recorded in 1536 well plate within minutes. The LDA shows 100% correct classification of all clusters and clear *ee*-dependent trends for all the five diols. Interestingly, the *S,S*-diethyl- and *S,S*-dimethyl tartrate show a high similarity at *ee* < 70% (at *ee* > 70% *S,S*-diethyl- and *S,S*-dimethyl tartrate show significantly different response). This is not unreasonable considering the high structural similarity of these compounds.

Following in this vein we also performed a quantitative analysis of the *ee* with mixtures of atorvastatin enantiomers. First, we used LDA to confirm a discriminatory potential of the FPBA-amine assemblies to distinguish various *ee* values (demonstrated by 100% classification and superior separation of the data clusters). The regression analysis using the support vector machine (SVM)[38] algorithm enables deconvolution of the multidimensional data to the actual *ee* values of (3*R*,5*R*)-atorvastatin and leave-one-out cross-validation approach validates the predictive potential of the developed model (see Supplemental Information). The plot of the predicted versus actual *ee* value for (3*R*,5*R*)-atorvastatin shows that the developed SVM model allowed simultaneous correct identification of two validation samples. The low prediction error (<2% *ee*) confirms the ability of the self-assembled system to correctly signal the levels of enantiomeric excess in complex molecules.
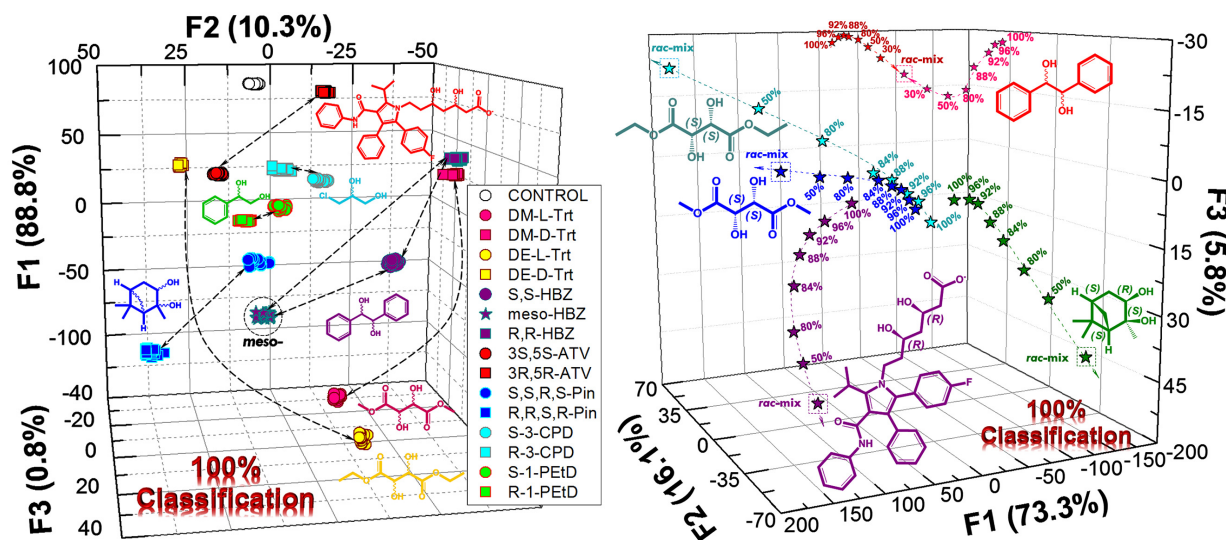
FULL PAPER

Figure 5. Graphical 3D outputs of LDA. **Left:** the results of qualitative LDA of various chiral diols. LDA output shows a perfect separation of the enantiomeric pairs and an excellent recognition capability with 100% correct classification of all 16 data-points corresponding to the individual analytes. The response space is defined by the first three factors (F1-F3) of LDA comprising 99.9% of total variance. **Right:** he result of the semi-quantitative LDA for simultaneous determination of *ee* of five diols. Clear *ee*-dependent trends in individual responses to each diol were identified. The response space is defined by the first three factors (F1-F3) of LDA comprising 95.2% of total variance.

The SVM confirms that the of L-tryptophanol based oxazolidine iminoboronate esters yield a highly sensitive and linear response that can be used to quantify the concentration, *ee* and absolute configuration of atorvastatin in a sample.

However, high throughput settings may require simple analysis method without using sophisticated statistical methods. Simplest method of obtaining absolute configuration and *ee* of reaction mixtures from fluorescence intensity (FI) is by utilizing a standard curve method. For our purpose, a standard curve is defined as a

graph of FI plotted on the Y axis, and various *ee* of standards along the X axis. The resulting graph of FI vs *ee* obtained by linear regression of points referring to FI readings from a number of mixtures of known *ee* used for calibration is linear (Figure 6). The absolute configuration and *ee* of controls (validation samples) and unknowns (for example asymmetric reaction samples) can be determined by interpolation of their fluorescence reading on the graph.
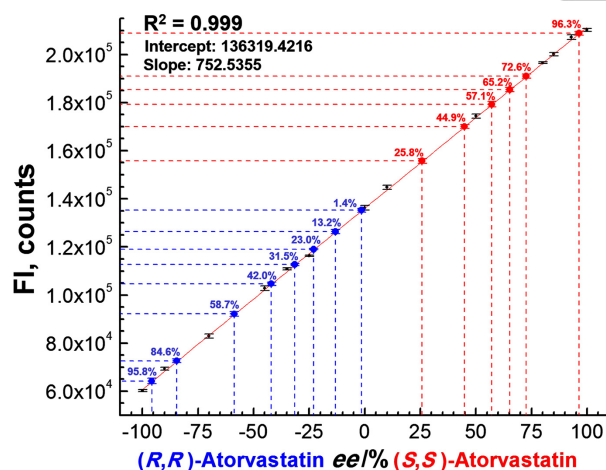

Figure 6. Standard curve obtained from L-tryptophanol-FPBA assembly (1:1, 40 µM) with atorvastatin enantiomers at various *ee* (black circle •). 14 samples of unknown atorvastatin enantiomer excess (blue and red circles) were simultaneously correctly analysed.

Table 2. The results of Atorvastatin *ee* determination using linear regression.

Entry	Actual		Fluorimetric Assay	
	Abs. config.	*ee*(%)	Abs. config.	*ee*[a] (%)
1	R,R	3	R,R	1.40
2	R,R	10	R,R	13.2
3	R,R	20	R,R	23.0
4	R,R	30	R,R	31.5
5	R,R	40	R,R	42.0
6	R,R	60	R,R	58.7
7	R,R	85	R,R	84.6
8	R,R	95	R,R	95.8
9	S,S	25	S,S	25.8
10	S,S	45	S,S	44.9
11	S,S	60	S,S	57.1
12	S,S	65	S,S	65.2
13	S,S	70	S,S	72.6
14	S,S	95	S,S	96.3

[a] Average value from two independent trials with 20 repetition in each trial.

Here, the linearity of the fluorescence response to atorvastatin *ee* suggests the estimation of the *ee* using standard curve will yield an excellent linear correlation. The standard samples were prepared using mixtures of the known *ee* of the atorvastatin

FULL PAPER

across a whole range of *ee* from pure (3*R*,5*R*)-atorvastatin to pure (3*S*,5*S*)-atorvastatin. Figure 6 shows the results of quantitative linear regression (R^2=0.999) between fluorescence intensity and *ee* of atorvastatin. This linear model was used to determine simultaneously 14 samples of unknown *ee* with excellent precision (Table 2).

Asymmetric reaction screening.

In general, there is a need to screen libraries of catalysts for their ability to yield products with high enantioselectivity. This requires time-efficient yet effective protocols for the systematic examination of crude products of asymmetric reactions in real time and in a HTS fashion. To illustrate the real-life utility of the present method, we decided to demonstrate the possibility of evaluating reaction mixtures of stereoselective reactions, both the yield and *ee* in small amounts (<1 mg) in crude form (without product crystallization) in high-throughput fashion.

As a benchmark for testing our method, we used the Noyori asymmetric transfer hydrogenation of benzils catalyzed by RuCl[(*R*,*R*)-Tsdpen](*p*-cymene) or RuCl[(*S*,*S*)-Tsdpen](*p*cymene) catalysts with a formic acid/triethylamine mixture, which affords *S*,*S*- and *R*,*R*-hydrobenzoin almost quantitatively with excellent diastereomeric and enantiomeric purity (Fig. 7).[9], [10]
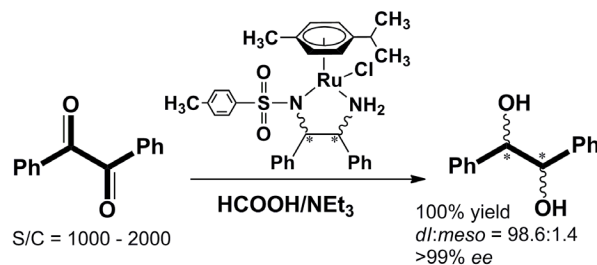

Figure 7. Noyori asymmetric hydrogenation of benzil with ruthenium catalyst yields hydrobenzoin in a high diastereomeric and enantiomeric purity.

Upon completion of the reaction, the products were divided into two portions, crude (after solvent evaporation; entry 2, 3, and 4), and a second portion was recrystallized from methanol (samples 2A; 3A; 4A). As a negative control, an incomplete reaction run without the presence of competent catalyst (entry #1 as a mixture of benzil, benzoin and inactive Ru-catalyst, not shown in Table 3) was also performed. For each entry, the absolute configuration and *ee* was determined using ¹H NMR[15] and compared to the results of the fluorimetric assay (Table 3).

Towards that end, we generated a calibration dataset using pure enantiomers of hydrobenzoin. The resulting multivariate data set was analyzed by SVM and 25 data points from the calibration set were used to develop/calibrate the linear regression model. The model was then validated using four independent samples (not part of the calibration dataset) and their *ee* was determined. The corresponding correlation graph (See SI) between the predicted *ee* and the actual *ee* is characterized by a regression (R^2) of 0.999842, 0.999818 and 0.999823 for calibration, cross-validation

and prediction respectively, with the root-mean-square errors (RMSEs) of calibration (C), cross-validation (CV), and prediction (P) below 1% *ee*.

Table 3. The results of benzil reduction.

| Entry | Ru-cat | ¹H NMR[a] | | HT Fluorimetric assay | |
		Abs. config.	*ee*(%)	Abs. config.	*ee*(%)[b]
2	*S*,*S*	*R*,*R*	97.5	*R*,*R*	95.4
2A	*S*,*S*	*R*,*R*	≥99	*R*,*R*	99.5
3	*R*,*R*	*S*,*S*	99	*S*,*S*	98.3
3A	*R*,*R*	*S*,*S*	≥99	*S*,*S*	99.7
4	*S*,*S* : *R*,*R*	*R*,*R*	4	*R*,*R*	3.75
4A	*S*,*S* : *R*,*R*	*R*,*R*	3.7	*R*,*R*	2.87

[a] Determined by ¹H NMR from multiple peaks integration. [b] Errors for determination of *ee* < 1%.

Next, the validated model was used to determine the *ee* in the six entries of unknown *ee* obtained from the Noyori reaction mixtures (Table 3). As expected, samples 2 and 2A (were prepared using RuCl[(*S*,*S*)-Tsdpen](*p*-cymene) catalysts), as well as samples 3 and 3A (prepared using RuCl[(*R*,*R*)-Tsdpen](*p*cymene)) were predicted as pure (*R*,*R*)-hydrobenzoin and (*S*,*S*)-hydrobenzoin respectively, and their *ee* were determined to be 95.4% *ee* for the crude product (entry 2), 99.5% *ee* for the recrystallized part (entry 2A), and 98.3% *ee* for the crude mixture (entry 3), 99.7% *ee* for the recrystallized sample (entry 3A), which is in perfect agreement with the ¹H NMR[15] results and literature values.[9]

Unknowns 4 and 4A were prepared using a 1:1 mixture of RuCl[(*S*,*S*)-Tsdpen](*p*-cymene) catalysts and RuCl[(*R*,*R*)-Tsdpen](*p*-cymene) catalysts, respectively, and gave a small excess of (*R*,*R*)-hydrobenzoin. The corresponding *ee* were predicted as 3.7% *ee* for the crude product (entry 4), and 2.8% *ee* for the recrystallized part of reaction mixture (entry 4A). To perform the *ee* assignment using the present method in 20 measurements per entry takes < 1 min. Each measurement requires only nanograms of the benzil substrate. Perhaps most importantly, the comparison of the results obtained for crude and crystallized samples shows that our method is not sensitive to traces of catalysts or reaction additives and may be applied to the determination of *ee* in crude product mixtures.

We have also tested sensitivity of the assay to the presence of *meso*-hydrobenzoin. It was found, that the method is not sensitive up to 5% of *meso*-form (See SI). Above this value, a new calibration set comprising *meso*-hydrobenzoin must be developed, and consequently, method could be used for simultaneous determination of *ee* and *de*.

As expected, the linearity of the fluorescence response to *ee* was also observed for the hydrobenzoin in a standard calibration procedure. This was first confirmed in the titration experiment (Figure 8, Left) as well as in a high throughput assay (Figure 8, Bottom). Both experiments provide almost identical dependence (Table 4) suggesting the validity of the high-throughput and standard curve approach.
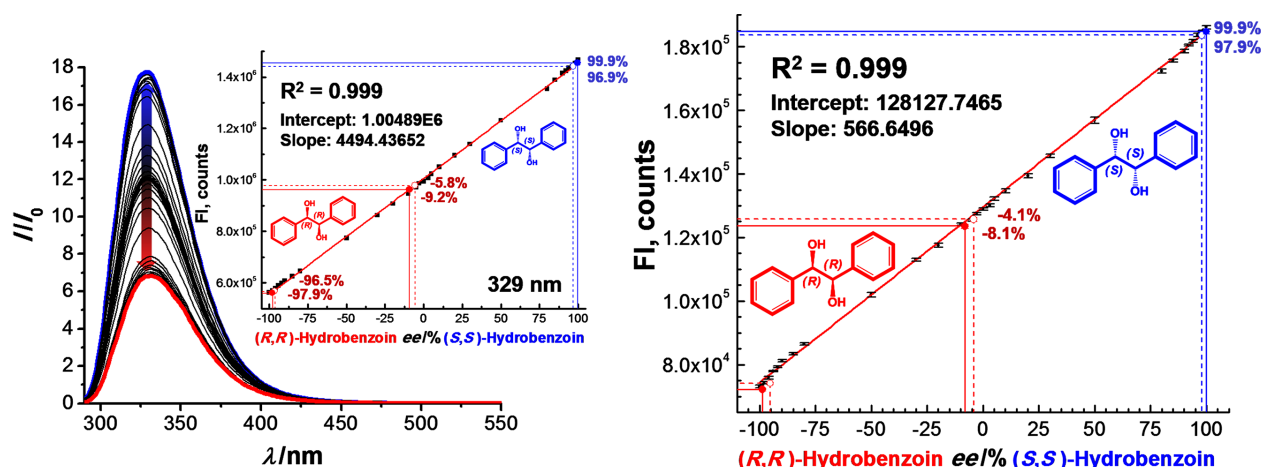
FULL PAPER

Figure 8. Standard curves generated from hydrobenzoin samples with various enantiomeric composition (*ee* range from 100% (*R,R*)-hydrobenzoin to 100% (*S,S*)-hydrobenzoin). **Left:** fluorescence titration profile of L-tryptophanol - FPBA (1:1, 40 *µ*M) with hydrobenzoin standards. Inset: Standard curve obtained for FI vs known *ee* used for calibration. Right: standard curve for FI readings from a number of mixtures of known *ee* used for calibration in HT fluorescence assay. Six unknown asymmetric reaction samples (four red circles, two blue circles), their absolute configuration and ee were simultaneously correctly determined.

Table 4. The results of benzil reduction from standard curve linear fitting.

		FI Titration [a]		HT Fluorimetric assay	
Entry	Ru-cat	Abs. config.	*ee*(%)[a] [c]	Abs. config.	*ee*(%)[b] [c]
2	*S,S*	*R,R*	96.5	*R,R*	95.3
2A	*S,S*	*R,R*	97.9	*R,R*	98.7
3	*R,R*	*S,S*	96.9	*S,S*	97.9
3A	*R,R*	*S,S*	99.9	*S,S*	99.9
4	S,S : *R,R*	*R,R*	5.8	*R,R*	4.1
4A	S,S : *R,R*	*R,R*	9.2	*R,R*	8.1

[a] Average value from two independent readings. [b] Average value from two independent trials with 20 repetition in each trial. [c] Errors for determination of *ee* < 2%

Because the tryptophanol based self-assembly depends both on the hydrobenzoin concentration and the change in *ee* value of the respective enantiomers, both can be calculated using artificial neural network (ANN).[39],[40] ANN utilizes a more complex and expanded calibration set that covers different total concentration values together with various *ee* in parallel with calibration set prepared using different unknown concentrations (Noyori asymmetric reaction outcomes). ANN was employed to calculate the total hydrobenzoin concentration and *ee* of the hydrobenzoin in Noyori asymmetric hydrogenation reaction mixtures (See Supplemental Information). The resulting data (Table S21 of SI) show that the known *ee* and concentrations are in perfect agreement with the data calculated by the artificial neural network (ANN) and that ANN using the fluorescence data obtained enable simultaneous determination of *ee* and hydrobenzoin concentration. This is, in part, due to the fact that benzil, as most of the aromatic ketones is not fluorescent. Thus, all the fluorescence in the reaction mixture originates from hydrobenzoin stereoisomers. This in turn means that the present method allows determination of the reaction yield even in reactions where the starting material is not fully converted to products.

Conclusions

In summary, we have demonstrated that the dynamic covalent self-assembly of an enantiomerically pure fluorescent amine reporter with 2-formylphenylboronic acid (FPBA) and a molecule containing a 1,2- or 1,3-diol moiety form diastereomeric complexes that display different fluorescence properties, an output signal measured using standard fluorescence plate reader in a high-throughput fashion. The chiral diol-induced changes in fluorescence are highly sensitive to the interplay between components of assembly, steric arrangement, and diol-receptor affinity. More importantly, these spectroscopic signatures are quantitatively related to the amount of analyte and absolute configuration. The ability to determine *ee* was tested on a set of 6 diol enantiomeric pairs including *meso*-hydrobenzoin, and anti-hypercholesterolemia drug atorvastatin. The qualitative study using the pattern recognition procedure (LDA) allowed for identification of all enantiomers tested. Likewise, the quantitative analysis of *ee* of atorvastatin confirmed the ability to quantify drug purity with an error in *ee* of <2% using a simple standard curve linear regression protocol. The final proof for the utility of the method was a high throughput determination of *ee* in reaction mixtures and products of Noyori asymmetric reduction of benzil to hydrobenzoin. Here, the tested (6 samples in 20 repetitions) and independently validated system was able to determine absolute configuration and *ee*, which was compared to the *ee* data obtained from NMR measurements. The error of the determination was < 1% *ee*. Finally, the artificial neural network (ANN) was employed for a simultaneous determination of *ee* and hydrobenzoin concentration. This experiment, was performed in a high-throughput fashion. Each reaction requires ca 10-20 ng/well of the benzil substrate and product mixtures can be analyzed in the same well. The present method enables measurement of *ee* in crude and crystallized samples, confirming that our method is not sensitive to traces of catalysts or reaction

FULL PAPER

additives. Together, the data presented here indicate that enantiopure tryptophan methyl ester/tryptophanol based assemblies are well suited for instant and accurate determination of the absolute configuration of chiral diols. These features are utilized in a simple, fast but also inexpensive way for monitoring the *ee* and total yield of diol enantiomers using a microscale HTS platform.

Experimental Section

Materials and methods

Starting materials, all reagents, and organic solvents were obtained from commercial suppliers and used without further purification.

Fluorescence.

Steady-state fluorescence emission and excitation measurements were recorded between 290 nm and 550 nm. Solution of L-tryptophanol and L-tryptophan methyl ester complexes were excited at 280 nm in spectrophotometric grade acetonitrile. The emission from probes was scanned in 1 nm step with appropriate excitation and emission monochromators band pass settings with dwell time 0.35 sec. under ambient conditions. Titration isotherms were constructed from changes in the fluorescence maximum at 330-335 nm.

Noyori asymmetric Ru catalyzed transfer hydrogenation of benzil.

Compounds 1, 2, 2A, 3, 3A, 4, 4A were prepared from the set of parallel asymmetric reductions of benzil catalyzed by RuCl[(*R*,*R*)-Tsdpen](*p*-cymene) or RuCl[(*S*,*S*)-Tsdpen](*p*-cymene) catalysts at 40°C with substrate/catalyst molar ratio (S/C) of 1500 in a DMF solution of $HCOOH/N(C_2H_5)_3$. Crude reaction products were divided in two parts, one portion of each sample was used without any further purification (sample 1; 2; 3; 4), and the second portion was recrystallized from methanol at -40°C (samples 2A; 3A; 4A).

Determination of association constants (Ka, M−1) by fluorescence titrations.

Then each reaction mixture has to be diluted 100 times with the same solvent to a final concentration of 40 μM and a final volume of 2 mL directly in a square quartz cuvette with 10mm path length. Titration isotherms (normalized fluorescence intensity vs concentration of diols) show the nonlinear least-squares best fits of the data to 1:1 binding model and yield association constants (K_a, M−1).

High-throughput array experiments design.

The array experiments were performed in 384 well density MATRICAL MP100-1-PS Microplates, and 1536 well density chemically resistant microplates MatriPlates MCR111-1-1, black and total working volume 120 μl and 5 μl respectively. The fluids were dispensed using a robotic high-precision 16-channel liquid handling system Nanodrop Express (BioNex Solution Inc.) with fixed-tip head 2x8 configuration. Each experiment was performed in 24 repetitions. For the control experiments an equal amount of acetonitrile was added instead of the chiral diol solutions. The printed plate was then incubated (3 min) and centrifuged to establish the equilibrium in the formation of diastereoisomeric iminoboronate/oxazolidine-boronate ester complexes. Plates were immediately read after incubation with a BMG PHERAstar Plus multi-mode microplate reader.

Data handling.

The response patterns associated with the sensor array are acquired in a form of multivariate data set. Raw data were subjected to the Student's t-test to exclude 4 data points out of 24 repetitions in order to examine the difference (standard deviation) between data within the set of repetitions. The coefficient of variability among the data within the class of 20 repetitions did not exceed 4% and obtained data were then analyzed using linear discriminant analysis (LDA) and artificial neural network (ANN) without any further pretreatment. Support vector machine (SVM) coupled with principal component analysis (PCA) and partial least squares (PLS) methods were applied for quantitative regression analyses of multivariate data sets. The training set was used to calibrate the model producing the root mean square error of calibration (RMSEC). The model was validated using 5-fold cross-validation producing the root mean square error of cross-validation (RMSECV). The validity and predictive ability of the developed model was then tested using independent data sets (validation samples). The predictive accuracy of a model was evaluated by the value of the root mean square error of prediction (RMSEP). The linear least squares method was used for finding the coefficients of polynomial equations that are a best linear fit to a set of X,Y data corresponding to *ee* and FI of the standards and unknown samples. A polynomial equation expresses the dependent variable Y (FI) as a first-order polynomial in the independent variable X (*ee*) generate a straight line (Y=*a*+*b*X, where *a* is the intercept and *b* is the slope), those coefficients (*a*, *b*) were used to predict values of X for each measured Y. In all these cases, Y is a linear function of the parameters *a* and *b*.

Accession Numbers

The accession number for the *meso*-hydrobenzoin, oxazolidine boronate ester complex reported in this paper is CCDC 1543343, and for the (*R*,*R*)-hydrobenzoin, oxazolidine boronate ester complex reported in this paper is CCDC 1543342.

Acknowledgements

[1]   R. N. Patel, *Coord. Chem. Rev.* **2008**, *252*, 659–701.
[2]   T. Hudlicky, A. J. Thorpe, *Chem. Commun.* **1996**, 1993.
[3]   H. C. Kolb, M. S. VanNieuwenhze, K. B. Sharpless, *Chem. Rev.* **1994**, *94*, 2483–2547.
[4]   J. Seyden-Penne, *Chiral Auxiliaries and Ligands in Asymmetric Synthesis*, Wiley, New York, **1995**.
[5]   T. P. Yoon, *Science* **2003**, *299*, 1691–1693.
[6]   Q.-L. Zhou, Ed. , *Privileged Chiral Ligands and Catalysts*, Wiley-VCH, Weinheim, Germany, **2011**.
[7]   K. B. Sharpless, K. Akashi, *J. Am. Chem. Soc.* **1976**, *98*, 1986–1987.
[8]   M. A. Andersson, R. Epple, V. V. Fokin, K. B. Sharpless, *Angew. Chem. Int. Ed.* **2002**, *41*, 472–475.
[9]   K. Murata, K. Okano, M. Miyagi, H. Iwane, R. Noyori, T. Ikariya, *Org. Lett.* **1999**, *1*, 1119–1121.
[10]   *Org. Synth.* **2005**, *82*, 10.
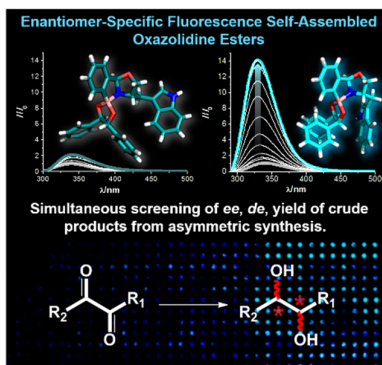[11]   Y. Chen, C. Chen, X. Wu, *Chem. Soc. Rev.* **2012**, *41*, 1742.

FULL PAPER

[12] D. Leung, S. O. Kang, E. V. Anslyn, *Chem Soc Rev* **2012**, *41*, 448–479.

[13] D. Parker, *Chem. Rev.* **1991**, *91*, 1441–1457.

[14] A. M. Kelly, Y. Pérez-Fuertes, S. Arimori, S. D. Bull, T. D. James, *Org. Lett.* **2006**, *8*, 1971–1974.

[15] A. M. Kelly, Y. Pérez-Fuertes, J. S. Fossey, S. L. Yeste, S. D. Bull, T. D. James, *Nat. Protoc.* **2008**, *3*, 215–219.

[16] S. L. Yeste, M. E. Powell, S. D. Bull, T. D. James, *J. Org. Chem.* **2009**, *74*, 427–430.

[17] K. W. Bentley, Y. G. Nam, J. M. Murphy, C. Wolf, *J. Am. Chem. Soc.* **2013**, *135*, 18052–18055.

[18] H. H. Jo, C.-Y. Lin, E. V. Anslyn, *Acc. Chem. Res.* **2014**, *47*, 2212–2221.

[19] E. A. Dragu, J.-V. Naubron, A. Hanganu, A. C. Razus, S. Nica, *Chirality* **2015**, *27*, 826–834.

[20] K. W. Bentley, D. Proano, C. Wolf, *Nat. Commun.* **2016**, *7*, 12539.

[21] W. H. Pirkle, T. C. Pochapsky, *Chem. Rev.* **1989**, *89*, 347–362.

[22] E. G. Shcherbakova, T. Minami, V. Brega, T. D. James, P. Anzenbacher, *Angew. Chem. Int. Ed.* **2015**, *54*, 7130–7133.

[23] E. G. Shcherbakova, V. Brega, T. Minami, S. Sheykhi, T. D. James, P. Anzenbacher, *Chem. - Eur. J.* **2016**, *22*, 10074–10080.

[24] M. Hutin, G. Bernardinelli, J. R. Nitschke, *Chem. - Eur. J.* **2008**, *14*, 4585–4593.

[25] Y. Pérez-Fuertes, A. M. Kelly, A. L. Johnson, S. Arimori, S. D. Bull, T. D. James, *Org. Lett.* **2006**, *8*, 609–612.

[26] E. Galbraith, A. M. Kelly, J. S. Fossey, G. Kociok-Köhn, M. G. Davidson, S. D. Bull, T. D. James, *New J Chem* **2009**, *33*, 181–185.

[27] A. Wilson, G. Gasparini, S. Matile, *Chem Soc Rev* **2014**, *43*, 1948–1962.

[28] B. W. McCrindle, L. Ose, A. D. Marais, *J. Pediatr.* **2003**, *143*, 74–80.

[29] P. Jones, S. Kafonek, I. Laurora, D. Hunninghake, *Am. J. Cardiol.* **1998**, *81*, 582–587.

[30] P. S. Sever, B. Dahlöf, N. R. Poulter, H. Wedel, G. Beevers, M. Caulfield, R. Collins, S. E. Kjeldsen, A. Kristinsson, G. T. McInnes, et al., *The Lancet* **2003**, *361*, 1149–1158.

[31] M. R. Law, *BMJ* **2003**, *326*, 1423–0.

[32] M. Korhonova, A. Doricakova, Z. Dvorak, *PLOS ONE* **2015**, *10*, e0137720.

[33] B. R. Krause, R. S. Newton, *Atherosclerosis* **1995**, *117*, 237–244.

[34] T. A. Kocarek, *Drug Metab. Dispos.* **2002**, *30*, 1400–1405.

[35] M. Otto, *Chemometrics: Statistics and Computer Application in Analytical Chemistry.*, Wiley-VCH, Weinheim; Cambridge, **1998**.

[36] R. G. Brereton, *Applied Chemometrics for Scientists*, John Wiley & Sons, Chichester, England ; Hoboken, NJ, **2007**.

[37] P. Anzenbacher, Jr., P. Lubal, P. Buček, M. A. Palacios, M. E. Kozelkova, *Chem. Soc. Rev.* **2010**, *39*, 3954.

[38] N. Cristianini, J. Shawe-Taylor, *An Introduction to Support Vector Machines: And Other Kernel-Based Learning Methods*, Cambridge University Press, Cambridge ; New York, **2000**.

[39] J. A. Burns, G. M. Whitesides, *Chem. Rev.* **1993**, *93*, 2583–2601.

[40] S. H. Shabbir, C. J. Regan, E. V. Anslyn, *Proc. Natl. Acad. Sci.* **2009**, *106*, 10487–10492.

FULL PAPER

Entry for the Table of Contents

FULL PAPER

Self-assembled fluorescent probes: incorporates chiral diols, allowing for simultaneous determination of *ee*, *de*, and product yields in a complicated matrix with only 10-20 ng/well of the substrate. Fluorescence is directly proportional to the absolute configuration and concentration of the diols. The applicability of this simple approach, demonstrated on the products of Noyori asymmetric hydrogenation of benzil and lipid-lowering drug atorvastatin in a highly parallel fashion with errors <1% *ee* confirming the feasibility of assaying crude products in real time, without any work up, as required for high-throughput screening.

Enantiomer-Specific Fluorescence Self-Assembled Oxazolidine Esters

Simultaneous screening of *ee*, *de*, yield of crude products from asymmetric synthesis.

Elena G. Shcherbakova, Valentina Brega, Vincent M. Lynch, Tony D. James, and Pavel Anzenbacher, Jr.*

High-Throughput Assay for Enantiomeric Excess Determination in 1,2- and 1,3-Diols and Direct Asymmetric Reaction Screening